GEOMETRIC AND RADIOMETRIC MODELS IN PROCESSING SPOT IMAGERY FOR OBJECT-SPACE SURFACES

J. Wu, M. J. Hsyu, C. H. Liu and D. C. Lin

Center for Space and Remote Sensing Research
National Central University
Chung-Li, Taiwan, ROC, 32054

XVII ISPRS Congress in Washington, D.C.
Comm. III , August 2-14, 1992

Abstract

For digital photogrammetry, an integrated approach to image matching and 3D positioning is proposed for stereoscopic SPOT images. The nonlinear functional models for space resection and the integrated approach are explicitly written down. Specifically, we use both piecewise linear models for time-dependent orientation parameters and a patchwise bilinear model for height parameters at elementary ground resolutions.

Our experiments show that fewer than 10 ground control points are more than enough to obtain in resection sub-pixel accuracies ± 7.2m, ± 4.6m and ± 5.5m in a local horizon coordinate system, respectively. The integrated approach can yield in one case a digital elevation model having ± 5m as a height root mean square error, when good approximations to terrain form and large weight constraints on heights are prerequisites.

Based on our experiences up to now, we review at the end our models and discuss their prospects.

Key Words: Space resection with SPOT imagery, Integrated image matching and 3D positioning.

1. INTRODUCTION

For analogue stereoscopic images, conjugate image points are best determined by an operator, e.g., on comparators. Of course, when the number of image points grows, working loads on the operator become very heavy. Thus, people have endeavoured to take full advantage of electronic computers to facilitate image correspondance processes since wide availability of digital images in early 1980's (e.g. Hannah, 1989). And least squares image matching is a representative algorithmic development (Ackermann, 1984). For digital stereo images, general practices follow a two-step solution by determining conjugate image points first and then by intersecting directional imaging rays to arrive at 3D point coordinates.

It is known that photogrammetric point positioning deals with geometric and radiometric distortions which result from taking optical pictures at different times and camera stations. When an analysis model takes perspective displacements, relief displacements and radiometric degradations all into account, the model becomes integral in nature and is more suitable for photogrammetric processing. Our proposed integrated approach to image matching and 3D positioning has been initially tested for aerial photos (Wu and Chang, 1990). Now the approach is applied to SPOT stereo images with a model extension that allows for time-varying characteristics of sensor's orientation along orbital paths.

While our interests in research on this topic are high, we feel motivated by engineers who desire up-to-date wide-coverage accurate height data for planning major governmental civil constructions.

2. MATHEMATICAL MODELS

2.1 Space Resection

Photogrammetric collinearity conditions used for SPOT panchromatic imagery with linear CCD arrays are:

$$x_i + a0_x + a1_x s_i + a2_x s_i^2 = -c\frac{a_{11_j}(X_i - X_{o_j}) + a_{12_j}(Y_i - Y_{o_j}) + a_{13_j}(Z_i - Z_{o_j})}{a_{31_j}(X_i - X_{o_j}) + a_{32_j}(Y_i - Y_{o_j}) + a_{33_j}(Z_i - Z_{o_j})} \quad (1a)$$

$$y_i + a0_y + a1_y y_i + a2_y y_i^2 = -c\frac{a_{21_j}(X_i - X_{o_j}) + a_{22_j}(Y_i - Y_{o_j}) + a_{23_j}(Z_i - Z_{o_j})}{a_{31_j}(X_i - X_{o_j}) + a_{32_j}(Y_i - Y_{o_j}) + a_{33_j}(Z_i - Z_{o_j})} \quad (1b)$$

where c : camera constant;

x_i, y_i : image coordinates of point i and $x_i = 0$;

s_i : strip coordinate in units of length or time;

$X_{o_j}, Y_{o_j}, Z_{o_j}$: time-dependent position parameters at sensor station j when point i is imaged;

$a_{11_j} ... a_{33_j}$: elements of an orthogonal matrix; they are functions of time-dependent attitude parameters $\omega_j, \phi_j, \kappa_j$;

X_i, Y_i, Z_i : object-space coordinates of point i;

$a0_x ... a2_y$: additional self-calibrating parameters.

In order to be practical for implementation, the time-dependent parameters of exterior orientation $X_{o_j}, Y_{o_j}, Z_{o_j}, \omega_j, \phi_j, \kappa_j$ are described by piecewise continuous linear models:

$$\begin{aligned} X_{o_j} &= (1 - s/d)X_{o_k} + (s/d)X_{o_{k+1}} \\ Y_{o_j} &= (1 - s/d)Y_{o_k} + (s/d)Y_{o_{k+1}} \\ Z_{o_j} &= (1 - s/d)Z_{o_k} + (s/d)Z_{o_{k+1}} \\ \omega_j &= (1 - s/d)\omega_k + (s/d)\omega_{k+1} \\ \phi_j &= (1 - s/d)\phi_k + (s/d)\phi_{k+1} \\ \kappa_j &= (1 - s/d)\kappa_k + (s/d)\kappa_{k+1} \end{aligned} \quad (2)$$

In Eq.(2) d is the separation between two neighboring sensor stations k and $k+1$; station j lies between k and $k+1$, and j is away from k in s units. For space resection, Eqs.(1,2) serve as our functional model in least squares adjustments. Based on weighted ground control points, we estimate mainly the position and attitude parameters $...X_{o_k}, Y_{o_k}, Z_{o_k}, \omega_k, \phi_k, \kappa_k...$ and the self-calibrating parameters.

2.2 Integrated Approach to Image Matching and 3D Positioning

The method of least squares image matching for stereo images can be written as

$$v''_{g'_i} = g'(x'_i, y'_i) - r_0 - r_1 g''(x''_i, y''_i); p''_{g'_i} \quad (3a)$$

in which g', g'' : gray-value functions evaluated at two corresponding image points x'_i, y'_i and x''_i, y''_i;

r_0, r_1 : radiometric additive and multiplicative parameters;

$v''_{g'_i}, p''_{g'_i}$: gray-value residual and its associated weight.

Logically and in a straitforward manner, the collinearity conditions Eqs.(1 with 2) can be used for pairs of image coordinates in Eq.(3a); and in vector notation, we get

$$v''_{g'_i} = g'(Z_i, \mathbf{p}', \mathbf{a}) - r_0 - r_1 g''(Z_i, \mathbf{p}'', \mathbf{a}); p''_{g'_i} \quad (3b)$$

where $\mathbf{p}', \mathbf{p}''$: vectors for position and attitude parameters along single- and double-prime orbital paths, respectively;

$\mathbf{a}$: vector for self-calibrating parameters.

In order to be feasible, height Z_i at the center of each ground resolution X_i, Y_i is described by patchwise continuous bilinear models:

$$Z_i = \frac{(X_{m+1} - X_i)(Y_{n+1} - Y_i)}{(X_{m+1} - X_m)(Y_{n+1} - Y_n)} Z_{m,n} + \frac{(X_i - X_m)(Y_{n+1} - Y_i)}{(X_{m+1} - X_m)(Y_{n+1} - Y_n)} Z_{m+1,n}$$
$$+ \frac{(X_{m+1} - X_i)(Y_i - Y_n)}{(X_{m+1} - X_m)(Y_{n+1} - Y_n)} Z_{m,n+1} + \frac{(X_i - X_m)(Y_i - Y_n)}{(X_{m+1} - X_m)(Y_{n+1} - Y_n)} Z_{m+1,n+1} \qquad (4)$$

Heights $\ldots Z_{m,n}, Z_{m+1,n}, Z_{m,n+1}, Z_{m+1,n+1} \cdots$ at nodes of a square grid are treated as primary unknown parameters in the combined Eqs.(3b,4).

In fact, $\ldots Z_{m,n} \ldots$ stand for the digital elevation model (DEM) we are interested in. So, we conduct iterative digital image matching by minimizing the weighted sum of squares of gray-value residuals and, simultaneously, arrive at object-space 3D point determination. For theories in a stricter sense that gray-value "truth" with each ground resolution is also asked for, readers can refer to among others Ebner and Heipke(1988) and Wrobel(1991).

3. EXPERIMENTS WITH SPOT IMAGERY

A stereoscopic SPOT image pair is selected for studying our models, see Table 1.

As far as the model for space resection with Eqs. (1,2) is concerned, we summarize accuracy results at 25 independent check points in Table 2. The number for dynamic sensor stations varies from 3 to 5. Ground control coordinates have throughout $\pm 50m$ a priori standard deviations while 6 additional self-calibrating parameters are treated as free parameters. Better accuracies result when 4 sensor stations are chosen, a plot of which is shown in Fig.1. We also see that cross-track accuracy in Y is better than along-track accuracy in X. This confirms the fact that SPOT imagery shows better cross-track geometric quality. When two ground control points lie between two adjacent sensor stations a solution for space resection can converge regularly, i.e. nonlinear Eqs. (1,2) are fulfilled in about 7 iterations to within $1.0 \times 10^{-5}[mm]$.

Space resection for SPOT stereo images yields the orientation parameters $\mathbf{p}', \mathbf{p}''$ and $\mathbf{a}$ for use in Eqs.(3b,4). The parameters are held fixed when performing experiments with respect to the model integrating image matching and 3D positioning. Our national $40 \times 40m^2$ digital terrain model (DTM) is derived from conventional aerial photographies using analytical plotters. Use of the DTM is made to interpolate heights for $20 \times 20m^2$ or $50 \times 50m^2$ grids. They represent reference heights adopted in comparison with heights estimated form SPOT sub-images, see upper left quadrants in Fig.2a. Table 3 reveals typical results on generation of digital elevation models. In general, the nonlinear functional relationship Eqs.(3b,4) can be satisfied at 95% to within 0.1 digital counts in 10 iterations. We notice that the integrated approach works for spaceborne images but weight constraints have to be imposed on the estimated height parameters. Extensive cases are still being studied. In particular, it is required to construct more reliable reference DEMs for accuracy analyses.

After geometric relationship between object-space elements and picture elements is reconstructed in a convergent solution, direct by-products out of the integrated approach are orthographic images. Fig.2a illustrates digital orthographic images. Their difference image and its histogram are shown in Fig.2b from which it is evident that the mean of differences in gray values is near zero and the distribution nearly Gaussian.

4. DISCUSSIONS

For SPOT imagery, our mathematical models used in space resection and in the integrated approach to image matching and 3D positioning are documented. In the course of our experiments, piecewise continuous linear modeling for time-dependent position and attitude parameters appears quite realistic when we consider the fact that SPOT stereo images of about 4° field of view have in our case 0.65 as a base-to-height ratio. SPOT scene CCTs contain orbital information, see CNES and SPOT Image(1988), which

Table 1. Brief description of a pair of panchromatic 1A images over central Taiwan from SPOT.

Base to height ratio :	0.65	
Heights above ground	827338 m	827271 m
Sensors on SPOT	HRV2	HRV1
Incidence angles	L10.4°	R24.1°
Data acquired on	15 Jan. 1987	16 Jan. 1987
Overlapping area :	57 km × 40 km	

Table 2. Accuracies in terms of root mean square errors in a local horizon system at 25 stationary check points.

		3 stations			4 stations			5 stations		
		Accuracies [m] at check points in								
		X	Y	Z	X	Y	Z	X	Y	Z
GCPs	25	6.83	4.66	7.20	7.16	4.51	5.17	7.43	4.72	5.64
	20	6.73	5.01	7.28	6.89	4.76	5.31	6.75	4.86	6.15
	15	6.97	5.69	7.48	7.41	5.05	5.59	6.46	5.03	6.63
	10	7.56	5.95	7.37	7.24	4.64	5.52	7.56	4.66	6.26
	6	8.25	5.26	7.81	7.54	5.95	6.32	11.59	67.48	148.10
	3	90.11	580.10	340.00	94.06	575.00	626.60	112.40	659.50	838.10

Table 3. Accuracies in height derived from the integrated model for image matching and 3D positioning (radiometric parameters r_0, r_1 in Eq.(3b) get little weighting; in the $1 \times 1 km^2$ test area maximum height difference $\Delta h_{max} = 81.49m$).

Height approximation using	terrain form given		average plane	
A priori standard deviations for heights	± 30m	± 5m	± 30m	± 5m
Height accuracies [m] by the integrated approach				
50 × 50 m grid (21 × 21 nodes)	16.39	8.61	16.58	11.56
20 × 20 m grid (51 × 51 nodes)	16.14	4.89	17.64	11.11

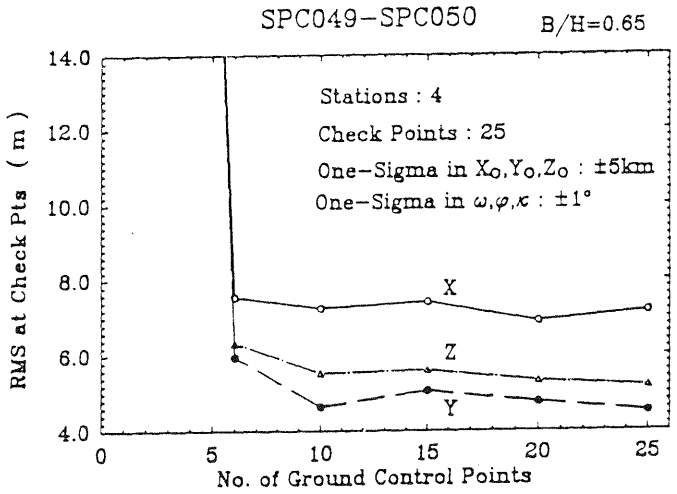

Fig.1. Plot of accuracies in X,Y,Z for 4 sensor stations (refer to Table 2).

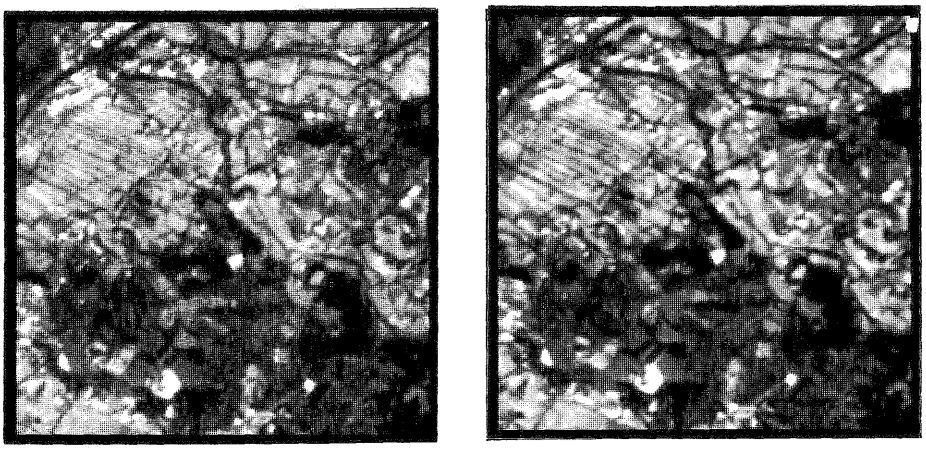

From the left SPOT subimage From the right SPOT subimage

Fig.2a. Orthographic images ($2 \times 2km^2$ in size; $50 \times 50m^2$ grid meshes; 41×41 grid nodes).

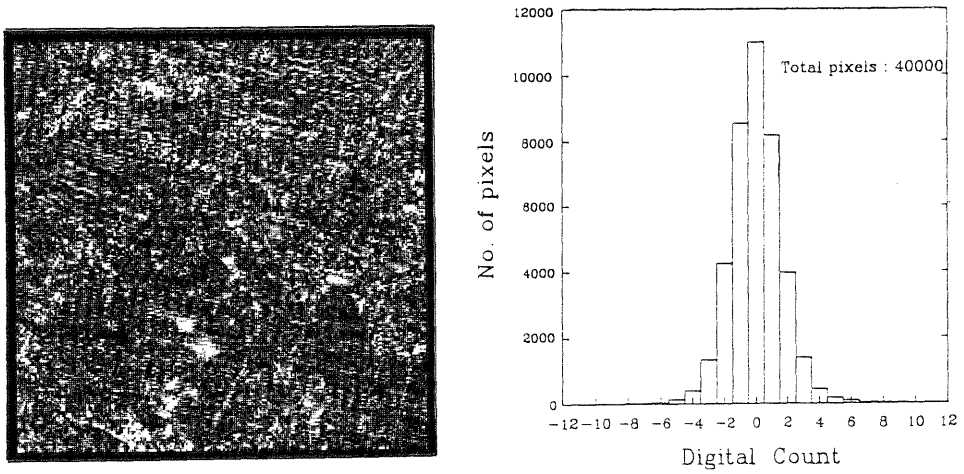

Fig.2b. Difference image (enhanced) between the two ortho-images in Fig.2a; shown to the right its histogram ($\sigma = 1.6078$ digital counts at 1 sigma).

is used by us to generate initial approximate orientation parameters along orbital paths. We conclude that fewer than 10 ground control points are quite enough for space resection (Chen and Lee,1990). It is interesting to note that the resection procedure is equally applicable to a single SPOT scene or to multiple scenes in stereoscopy. As far as improvements on additional self-calibrating parameters are concerned more research on our part is necessary.

One of the purposes in studying our integrated model for image matching and 3D positioning is to test its applicability to spaceborne stereo imagery. We know there is an advantage in theoretical analysis on error propagation; it is a worthy trade-off when thinking about rather heavy computational loads. Another advantage inherent in the integrated approach is automatic generation of orthographic (sub-)images along with that of a dense digital elevation model. Currently, we must impose weights in form of a diagonal matrix on unknown height parameters of DEMs. This arises in part from the fact there exists locally no or little image contrast in SPOT sub-images. Therefore, our on-going research efforts are led to

- determine in image preprocessing weighting functions that allow for gray-value contrast, textures or features in (sub-)images;
- design regional radiometric parameters to replace two global parameters r_0, r_1 in Eq.(3b);
- discover methods of interpolation more realistic than those by non-differentiable, continuous piecewise linear or patchwise bilinear modeling;
- as a long-term goal correct radiometrically for atmospheric effects and terrain effects to arrive at normalized reflectance images for photogrammetric multi-point positioning.

At last, we kindly acknowledge the research funds provided by the Sinotech Foundation for Research and Development of Engineering Sciences and Technologies.

5. REFERENCES

Ackermann, F.,1984. High precision digital image correlation. Proc. of the 39th Photogrammetric Week, Stuttgart, pp.231-243.

Chen, L.C. and Lee, L.H., 1990. A systematic approach to digital mapping using SPOT satellite imagery. Journal of the Chinese Institute of Civil and Hydraulic Engineering 2(1), pp.53-62.

CNES and SPOT Image, 1988. SPOT users' handbook. Volumes 1 and 2.

Ebner, H. and Heipke, C., 1988. Integration of digital image matching and object surface reconstruction. Int. Arch. Photogramm. Remote Sensing 27(B11), pp.III-534 to III-545.

Gruen, A.W. and Baltsavias, E.P., 1987. High-precision image matching for digital terrain model generation. Photogrammetria 42, pp.97-112.

Hannah, M.J., 1989. A system for digital stereo image matching. Photogrammetric Engineering and Remote Sensing 55(12), pp.1765-1770.

Heipke, C., 1992. A global approach for least-squares image matching and surface reconstruction in object space. Photogrammetric Engineering and Remote sensing 58(3), pp.317-323.

Rosenholm, D., 1987. Multi-point matching using the least-squares technique for evaluation of three-dimensional models. Photogrammetric Engineering and Remote Sensing 53(6), pp.621-626.

Westin, T., 1990. Precision rectification of SPOT imagery. Photogrammetric Engineering and Remote Sensing 56(2), pp.247-253.

Wrobel, B.P.,1991. Least-squares methods for surface reconstruction from images. ISPRS J. Photogramm. Remote Sensing 46, pp.67-84.

Wu, J. and Chang, J.H., 1990. An algorithm for point positioning on digital images and in object space. Int. Arch. Photogramm. Remote Sensing 28(5/2), pp.1196-1202.